

High-Throughput Satellite Connectivity for the Constant Contact Vehicle

Ryan A. Stevenson^{#1}, David Fotheringham^{#2}, Tom Freeman^{#3}, Turner Noel^{#4}, Tim Mason^{#5}, Shahram Shafie^{#6}

[#]Kymeta Corporation, USA

{¹ryan, ²dfotheringham, ³TomF, ⁴tnoel, ⁵tmason, ⁶sshafie}@kymetacorp.com

Abstract — The modern automobile is an artificial intelligence computer requiring constant contact with data networks to upload vehicle data and maintain the processing platform with software and firmware updates. 5G roll-out must include non-terrestrial networks (NTNs) to augment terrestrial cellular networks and achieve constant contact. We have commercialized a satellite vehicle terminal based on a novel, flat-panel, electronically scanned, metamaterials antenna technology (MSAT) that makes high-throughput satellite connectivity to the consumer automobile a practical reality.

Keywords — Electromagnetic metamaterials, satellite antennas, mobile antennas, leaky wave antennas, low earth orbit satellites, 5G mobile communication.

I. INTRODUCTION

The modern automobile, beyond simply being a conveyance, is an artificial intelligence (AI) system that performs massive sensor fusion and deep learning to completely understand its environment and make driving decisions autonomously. To accomplish these functions, today's vehicle is comprised of over 150 different electronic subsystems controlled by some type of processor or microcontroller [1]. Collectively these processing systems utilize over 100 million lines of software code [2]. Companies like NVIDIA are now producing AI-enhanced computers, specifically for connected cars, that are capable of over 320 tera-operations per second (TOPS) [3].

Maintaining these processing platforms with software updates and improving vehicle safety and the driving experience requires the vehicle to be in constant contact with data networks. 5G terrestrial networks alone are unsuited to meet this need due to restricted geographic coverage and capacity limitations [4]. 3GPP anticipates that satellite-based, non-terrestrial networks (NTNs) will augment 5G terrestrial networks for mobile platforms [5], however the typical user equipment required to establish a satellite link to a moving automobile (typically consisting of a gimbaled dish antenna) has, until now, made the idea completely unapproachable. In addition, a satellite user terminal with a production cost and volume commensurate with automotive industry demands, where 93,856,388 vehicles were sold in 2016 globally, has never been achieved [6]. Other key performance metrics for a practical, in-board mounted, vehicle satellite terminal are shown in Table 1.

Table 1. Key performance metrics for a practical vehicle satellite terminal

Feature	Requirement	Description
Data Throughput	> 10 Mbps	Two-way VOIP, multi-cast content, HD video
Tracking Rate	> 15 degrees/sec	Track through typical driving maneuvers
Profile	< 2.5 cm thick	Interior mounting flush to the roof line
Weight	< 5 Kg	Safe mounting in the roof
Power	< 100 W @ 12 VDC	Compatible with vehicle power delivery system
Temperature	-40° C to +80° C (+105° C)	Operational (survivable) temperature range
Reliability	Automotive grade	10-year useful life typical

We have addressed these critical requirements by commercializing a novel, electronically-scanned antenna technology based on a diffractive metamaterials concept, called Metamaterial Surface Antenna Technology (MSAT). Electronic scanning is achieved with high-birefringence liquid crystals. The use of liquid crystals (LC) as a tunable dielectric at microwave frequencies permits large-angle (>75°) beam scanning and fast tracking (~30°/sec), with power consumption of ~30 Watts, antenna thickness ~ 2.5 cm, and no moving parts. Our approach, using LC and optimizing the design for compatibility with liquid crystal display (LCD) fabrication processes, positions the technology for mass production by leveraging the manufacturing infrastructure of the LCD industry.

II. METAMATERIAL SURFACE ANTENNA TECHNOLOGY

A. Holographic Metasurfaces

Recently, three-dimensional, refractive metamaterial approaches have been extended to two-dimensional surfaces, or metasurfaces [7]. Metasurfaces have several advantages over traditional bulk metamaterials, namely that they take up less physical space and have the potential for less-lossy structures. Metasurfaces are characterized by both the periodicity of scatterers and thickness of the surface being small relative to the wavelength of interest. We are leveraging the metasurface concept, in conjunction with diffractive beamforming principles to commercialize MSAT [8].

In the MSAT approach the metasurface is introduced along one of the surfaces of a guided-wave feed structure, as shown

in figure 1, such that the scattering elements are weakly coupled to the feed wave. In this example the metasurface is placed along the broad wall of a rectangular waveguide.

$$\begin{pmatrix} D_z \\ D_y \\ D_x \end{pmatrix} = \begin{pmatrix} \epsilon_{\parallel} & 0 & 0 \\ 0 & \epsilon_{\perp} & 0 \\ 0 & 0 & \epsilon_{\perp} \end{pmatrix} \begin{pmatrix} E_z \\ E_y \\ E_x \end{pmatrix} \quad (1)$$

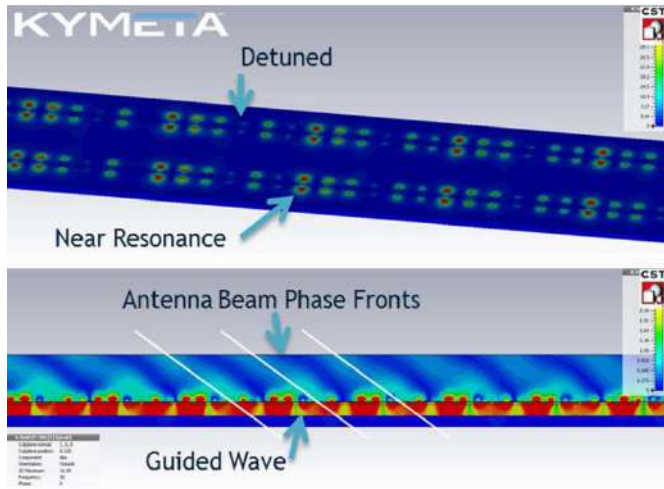


Fig. 1. Top view and cross section showing the metasurface, feed structure, and the antenna beam produced from the holographic diffraction of the guided feed wave against the metasurface.

Figure 1 shows that the scattering elements in the metasurface radiate with a periodicity corresponding to the scan angle of the beam. In other words, elements that are in-phase to produce coherent radiation at the desired scan angle are tuned to scatter strongly, while elements that are out of phase for the given scan angle are detuned so as not to radiate. The scattering strength of each element is determined through a holographic diffraction calculation as described in [9].

A critical factor with MSAT is that the diffraction pattern on the metasurface is produced through the tuning of element resonances, but the antenna beam is not produced *on* a resonance. Thus, the antenna bandwidth is not limited by the resonance of the elements but by the tunability of the elements (change in resonant frequency). MSAT, therefore, can achieve broadband operation as required for high-throughput satellite communications.

B. Liquid Crystal Display Manufacturing

MSAT employs high-birefringence, nematic liquid crystals as a tunable dielectric to control the capacitance of the metasurface scattering elements. The relative permittivity tensor, shown in equation 1, defines a uniaxial system where the permittivity varies between a perpendicular value and a parallel value, depending on the tuning state of the scattering elements. A bias voltage applied to the scattering elements causes the LC molecules to rotate from the perpendicular orientation to the parallel orientation. This rotation increases the LC relative permittivity, thereby increasing the capacitance of the scattering element and detuning the resonance frequency.

The metasurface construction, with an upper and lower substrate/electrode and LC as the tunable medium disposed in between, closely resembles the stack-up of an LC display. Array elements are individually addressed in an active matrix addressing scheme using printed thin film transistors (TFTs) exactly as typical displays are made. Active matrix addressing in combination with LCD lithography capability means that both receive and transmit antenna elements can be interleaved, and independently operated on the same substrate.

C. MSAT Performance and Trade-offs

MSAT trades off discrete amplitude and phase control of each antenna element, as with phased array, for the manufacturability and cost of the diffractive metasurface approach. While dramatically lowering cost and power consumption over phased array and achieving consumer electronics scale manufacturing, MSAT has also demonstrated noteworthy technical capabilities for a flat-panel, electronically scanned antenna:

- Full duplex receive/transmit from a single physical aperture
- Dynamically adjustable polarization from tracking linear to circular (RHCP and LHCP)
- Full 360° azimuth scanning and elevation scanning below 15° with return loss independent of scan angle
- Compliance with ITU and FCC power spectral density (PSD) masks

Figure 2 shows a broadside beam pattern for our Ku-band 70 cm antenna at 14.25 GHz, where compliance against the ITU mask is shown without power back-off. Broadside performance achieves a dynamic bandwidth of 1 GHz on receive (11.4-12.4 GHz), instantaneous bandwidth > 100 MHz, and peak G/T of 9.5 dB/K.

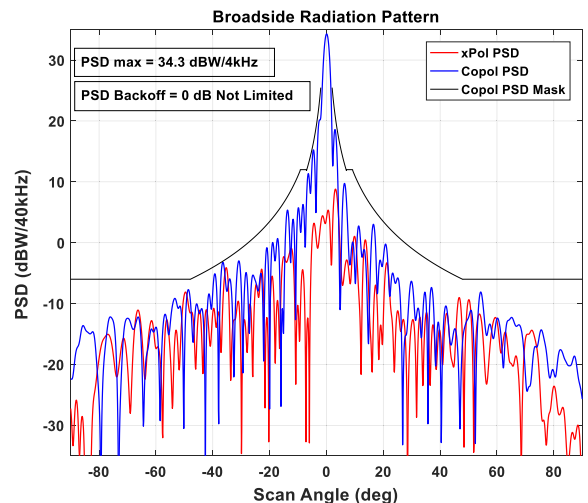


Fig. 2. Broadside co-polarization and cross-polarization beam patterns for the 70 cm Ku-band antenna shown with the ITU mask overlaid.

Electronically scanned antennas exhibit additional trade-offs in performance due to scan loss and beam broadening. These degradations result from the projected aperture area decreasing with increasing scan angle. This effect can be seen in figure 3, where beam pattern plots shown with varying scan angle demonstrate a $\cos^{1.2}(\theta)$ roll-off. In addition, the half-power beam width is also observed to increase from 1.75° to 5° , as measured along the direction of scan. Beam broadening will impact PSD mask compliance and system throughput depending on the geographic location of the satellite terminal relative to the satellite longitude.

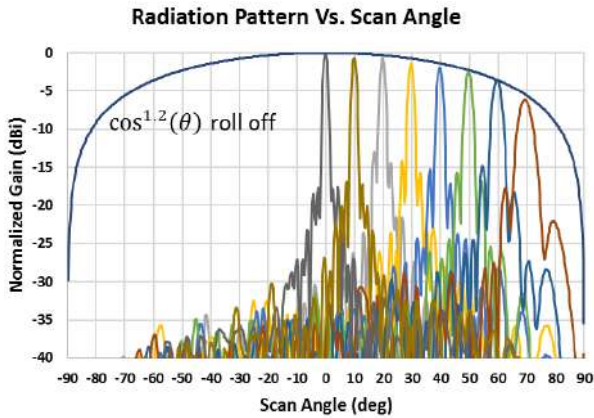


Fig. 3. Scan loss and beam broadening as a function of scan angle

III. INTEGRATED VEHICLE TERMINAL

The integrated vehicle terminal is shown schematically in figure 4. Because the antenna subsystem module (ASM) combines both receive (Rx) and transmit (Tx) functions, a diplexer is placed at the input of the antenna to isolate Rx and Tx paths between the low-noise block downconverter (LNB) and the block upconverter (BUC). Between the antenna itself and the diplexer > 100 dBc of isolation is achieved between Rx and Tx paths. Following the LNB, a 10 dB coupler provides an Rx intermediate frequency (IF) signal to an on-board tracking receiver while the primary Rx IF signal is routed to the system modem. The Tx path follows the BUC, through the diplexer, and into the antenna.

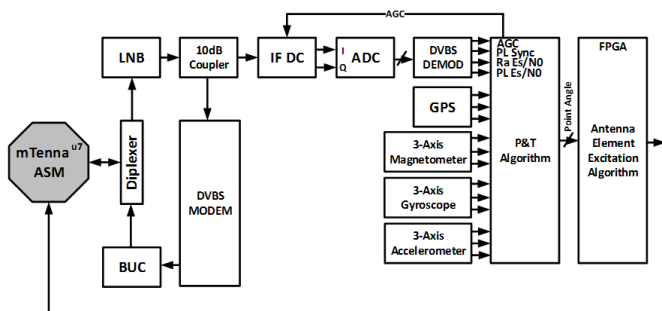


Fig. 4. A block diagram of the integrated vehicle terminal

A critical requirement for a vehicle satellite terminal is the ability to track the desired satellite and point the Rx and Tx beams accurately on a highly-dynamic platform, but doing so with a low-cost solution. The vehicle terminal tracking

subsystem uses inexpensive components including a GPS receiver, low-cost, MEMS-based, accelerometer, gyroscope, and magnetometer and a baseband receiver that provides Es/No estimates of the received signal.

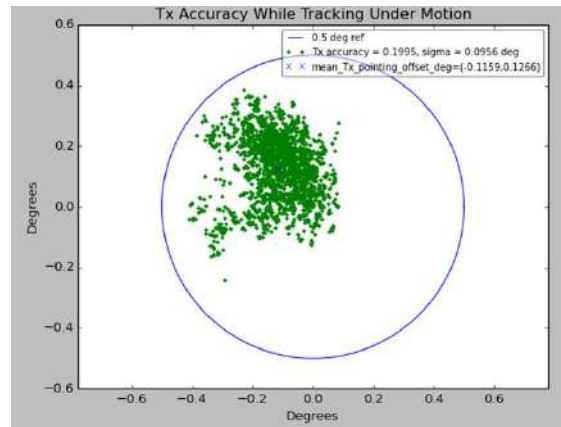


Fig. 5. Tx pointing accuracy results for absolute platform motion of +/- 10 degrees at 15 degrees/sec and beam scan angle of 40 degrees.

Closed-loop feedback is accomplished with a hill climbing algorithm that dithers the Rx beam and converges in the direction of increasing Es/No. The tracking algorithm separately peaks the pointing angle (theta and phi) as well as the polarization angle. The angle rate data from the gyroscope is used to correct the attitude solution after detected rotations. The Tx array is then pointed independently using the best tracking solution.

Figure 5 shows Tx pointing error measurements for absolute platform motion of +/- 10 degrees at an angular rate of 15 degrees/sec. These results were obtained at a beam scan angle of 40 degrees. The mean pointing error is roughly 0.2 degrees, with all measurement points falling within 0.5 degrees of pointing error.

IV. SATELLITE COVERAGE AND THROUGHPUT

Geographic coverage and data throughput depend heavily on the characteristics of the space segment, as well as the performance characteristics of the antenna and vehicle terminal. The generation of satellite and the location of the terminal relative to the satellite will impact the coverage area and throughput.



Fig. 6. SNR coverage map for the 70 cm vehicle terminal operating on IS-17

While scan loss has a straightforward link impact, beam broadening only occurs in the direction of scan. For a terminal located due East or West the beam elongates along the geostationary arc (skew of 90 degrees). This is a worst-case condition where the RF power to the terminal may need to be backed off to compensate for the beam broadening and comply with regulatory PSD limits. If the terminal is due North or South of the target satellite, the beam elongation is perpendicular to the geostationary arc (skew of 0 degrees), hence the beam widening will not impact adjacent satellites.

Figure 6 demonstrates the effect of skew for the 70 cm terminal operating with a scan angle of 50° and skew angle of 20° on Intelsat IS-17 at 66° East (a legacy wide-beam satellite). The SNR contours for 0 dB SNR and 7 dB SNR are shown for a scenario where no PSD back-off is applied. These contour lines are overlaid on a colormap of SNR contours determined for the appropriate PSD back-off per the scan/skew condition. Significant reductions in coverage area can be seen due to the PSD back-off required because of beam broadening and scan loss at this scan/skew condition.

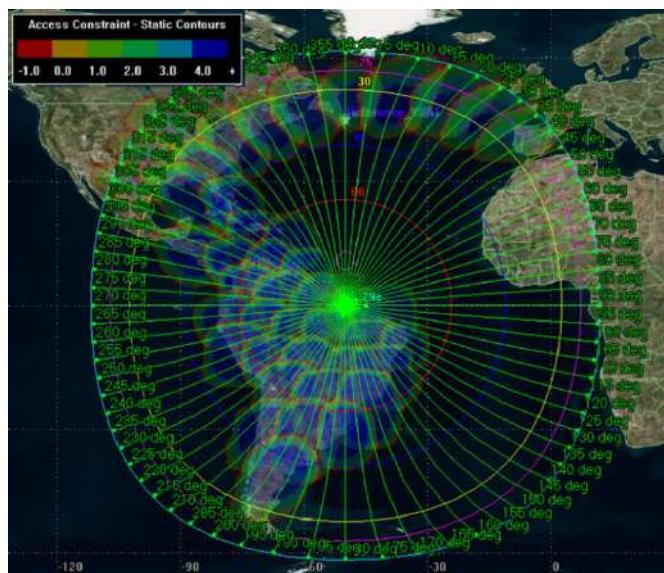


Fig. 7. Coverage map for the 70 cm integrated terminal operating on IS-29E.

Coverage and throughput improve tremendously when considering operation on the next generation of high-throughput satellites (HTS), e.g., IS-29E, part of the Intelsat EPIC^{NG} constellation. Figure 7 demonstrates the improved coverage and SNR on IS-29E, where the regional spot beams provide consistent coverage over a wide swath of territory.

MSAT provides a scalable solution depending on the data throughput desired. As demonstrated in table 2 (assuming a DVB-S2 waveform), a 70 cm diameter aperture can deliver 10 Mbps operating on a GEO-HTS satellite. A 20 cm aperture can deliver upwards of 100 Mbps, while mobile, when paired with the next generation low earth orbit (LEO) satellite networks. A 40 cm radial antenna can deliver an at-home equivalent internet experience anywhere the vehicle goes.

Table 2. Example forward link data rates for 20 cm/LEO and 70 cm/GEO-HTS use cases

Parameter	70 cm/ HTS	20 cm/LEO	
Usable Bandwidth	7.2	54	MHz
Tx EIRP	39.6	33.8	dBW
Path Loss	204.8	175.4	dB
Rx Gain	33.5	28.58	dBi
Received Power	-131.83	-119.03	dBW
Noise Power	-136.05	-127.30	dBW
C/N	4.22	8.27	dB
DVB-S2 MODCOD	QPSK 3/4	8PSK 2/3	
Spectral Efficiency	1.39	1.88	bps/Hz
Data Rate	10.01	101.52	Mbps

V. CONCLUSION

We have demonstrated a high-throughput satellite communications terminal that address the key performance requirements of the consumer automobile. By solving the challenges typically associated with satellite tracking terminals, MSAT makes satellite connectivity practical to implement for the constant contact vehicle. This capability complements 5G terrestrial service and provides automobile manufacturers with the ability to offer constant connectivity in a hybrid approach that is practical for today's GEO constellations and scalable to future LEO constellations.



Fig. 8. The 70 cm integrated terminal installed in the roof of a Toyota Land Cruiser.

REFERENCES

- [1] B. O'donnell. (2016). USA Today website. [Online]. Available: <https://www.usatoday.com/story/tech/columnist/2016/06/28/your-average-car-lot-more-code-driven-than-you-think/86437052/>
- [2] K. Abhimanyu. (2016). Techcrunch.com website. [Online]. Available: <https://techcrunch.com/2016/08/28/how-connected-cars-are-turning-into-revenue-generating-machines/>
- [3] (2018). NVIDIA website. [Online]. Available: <https://www.nvidia.com/en-us/self-driving-cars/drive-px/>
- [4] Siegele, Ludwig, "The World in 2018," The Economist, pp. 126, 2018
- [5] "Study on New Radio (NR) to Support Non-Terrestrial Networks (Release 15)", 3GPP TR 38.811 v.0.2.1, November 2017
- [6] (2018). OICA website. [Online]. Available: <http://www.oica.net/wp-content/uploads/total-sales-2016.pdf>
- [7] C.L. Holloway, E.F. Keuster, J.A. Gordon, J. O'hara, J. Booth, and D.R. Smith, "An Overview of the Theory and Applications of Metasurfaces: The Two-Dimensional Equivalents of Metamaterials," IEEE Ant. Prop. Mag., Vol. 54, No. 2, pp. 10-35, 2012.
- [8] K.M. Palmer, "Intellectual Ventures Invents Beam-Steering Metamaterials Antenna," IEEE Spectrum, November 30th, 2011.
- [9] M.C. Johnson, S.L. Brunton, N.B. Kundtz, J.N. Kutz, "Sidelobe Canceling for Reconfigurable Holographic Metamaterial Antenna," IEEE Trans. Ant. Prop., Vol. 63, No. 4, pp. 1881-1886, 2015.